Environ Geol (2006) 51: 309–323
DOI 10.1007/s00254-006-0328-8

ORIGINAL ARTICLE

Elias Dimitriou
Ierotheos Zacharias

Groundwater vulnerability and risk mapping in a geologically complex area by using stable isotopes, remote sensing and GIS techniques

Received: 6 February 2006
Accepted: 4 May 2006
Published online: 3 June 2006

E. Dimitriou (✉)
Hellenic Centre for Marine Research,
Institute of Inland Waters,
P.O. Box 712, Mavro Lithari,
Anavissos Attikis 19013, Greece
E-mail: elias@ath.hcmr.gr
Tel.: +30-229-1076389
Fax: +30-229-1076323

I. Zacharias
Department of Environmental
and Natural Resources Management,
University of Ioannina, 2 Seferi Str.,
30100 Agrinio, Greece
E-mail: izachari@cc.uoi.gr

Abstract Groundwater vulnerability and risk mapping is a relatively new scientific approach for facilitating planning and decision making processes in order to protect this valuable resource. Pan European methodology for aquifers vulnerability has recently been developed by assessing all the existing relevant techniques and emphasizing on karstic environments. In the particular study, state-of-the-art methods and tools have been implemented such as remote sensing, isotopic investigations and GIS to map the groundwater vulnerability and pollution risk in a geologically complex area of W. Greece. The updated land use map has been developed from a Landsat 7+TM image elaborated with image analysis software, while the detailed hydrogeologic properties of the area have been recorded with an intensive isotopic study. The local groundwater vulnerability map has been produced following the aforementioned Pan European method, in a GIS environment while the risk map, which was the final product of the study, has been developed after combining the vulnerability and the land use maps. The results indicated that the areas comprised of highly tectonized calcareous formations represented high vulnerability and risk zones while forested areas away from the karstic aquifer illustrated moderate to low vulnerability. Moreover, human activities increase the pollution risk in lowland areas consisting of sedimentary deposits that have been classified as moderate vulnerability. The particular methodology operated efficiently in this study and due to its accuracy and relatively easy implementation can be used as a decision support tool for local authorities.

Keywords Groundwater · Vulnerability · Hydrogeology · Karst · Greece

Introduction

Groundwater resources and particularly karst aquifers comprise very important suppliers of freshwater to both humans and ecosystems. Nevertheless, they are considered to be vulnerable to pollution mainly due to anthropogenic activities such as agriculture and waste disposal. Groundwater vulnerability mapping is a relatively new scientific approach initially appearing in the late 1960s (Adams et al. 2003) and significantly progressing during the last decade through the improvement of hydrologic models, GIS and other cartographic tools (Dixon 2005). Groundwater vulnerability term incorporates both the concepts of intrinsic and specific aquifers' vulnerability. Intrinsic vulnerability is based on the fact that the physical environment offers a specific level of protection to the aquifers depending mainly on the hydrogeologic and geomorphologic conditions of an

area while specific vulnerability considers additionally the properties of a particular contaminant (Vrba and Zaporozec 1994).

The legislative framework in many countries today reveals the need for groundwater vulnerability and risk assessment. Water framework directive (EC/2000/60) in European Union refers indirectly to the evaluation of aquifers' vulnerability since it requires an initial characterization of all the groundwater bodies in the member states with respect to their pollution risk. The under discussion EU groundwater directive will possibly enforce groundwater vulnerability assessment on a European level since it demands application of the precautionary principle in groundwater bodies and examination of the relationship between the surface and the underground water resources as well as the quantification of potential human pressures on them (EU/2003/0210).

Assessing vulnerability in karstic aquifers incorporates significant difficulties due to their particular structural characteristics that are dominated by heterogeneity and anisotropy. Moreover, their exact boundaries can be very much extended and hard to define while features such as the epikarst zone and dual porosity (fractures and conduits) constraint the quantification of pollution risk (Adams et al. 2003). Furthermore, groundwater risk evaluation and management, which is an important responsibility of environmental authorities today, requires detailed assessment of aquifers' vulnerability and estimation of potential hazards from human activities. Therefore, the implementation of preventive or mitigation measures regarding potential contamination events depends mostly upon the accurate quantification of groundwater vulnerability and the possible impacts from the overlying land uses.

Extensive research has been conducted for the development of multiple methodologies on groundwater vulnerability mapping and risk assessment that could operate efficiently under different environments (Goldscheider et al. 2000; Jeannin et al. 2001; Vias et al. 2002; Babiker et al. 2005). However, most of these approaches present particular advantages in certain aspects of the process and drawbacks in other elements such as data requirements, implementation scale, detail of analysis and subjectivity that often lead to high uncertainties in the results. Recently, a European program (Cost action 620) attempted to produce a Pan European method for groundwater vulnerability and risk mapping by assessing and elaborating all the relevant existing methodologies (Adams et al. 2003). The outcome of this effort is a scientific technique that has specific advantages in relation to several preexisting methods, requiring detailed hydrogeologic and land use information. This prerequisite can be well satisfied today through isotopic studies that comprise a common practice, especially in karstic areas where classical scientific approaches are often inefficient regarding groundwater flow tracing and recharge areas identification (Finch 1997; Hussain et al. 1999; Jones and Banner 2003; Diazconti et al. 2003; Swarzenski et al. 2001). Remote sensing and advanced processing tools can also facilitate accurate and high resolution land use mapping.

In this study, state-of-the-art techniques such as isotopic hydrology, GIS and remote sensing have been implemented to apply a groundwater intrinsic vulnerability and risk mapping effort for the area hosting the largest natural lake in Greece, Trichonis Lake, which is also included in the Natura 2000 European network of protected sites. The aim of the current study was to test whether the aforementioned Pan European method for groundwater intrinsic vulnerability and risk mapping is applicable to the environmental conditions of the study area (complex geology and semi arid climate) and assess its potential as a decision support system in resource planning and management.

Description of the study area

The study area that covers the broader area of Trichonis lake catchment, which is located in W. Greece, has an extent of approximately 730 km^2 and hosts a deep and large water body, Trichonis lake, with a surface of 97 km^2 and a maximum depth of 58 m. The hydrogeologic properties of the area are complex (Fig. 1), since the most commonly encountered formation is low to medium weathered limestone (covers 31% of the total catchment area) that is highly tectonized and presents well developed folds, faults and karst phenomena. This particular geologic formation contributes significantly to the development of preferential groundwater flows and provides submerged springs in Trichonis lake. Low permeability flysch formations are observed in the southern and western parts of the study area while Quaternary and Pleistocenic sediments are encountered around the lake (Fig. 1). Important water bodies outside the lake's catchment that can interact with it are Evinos river (East) and Fidakia stream (North) that also flow on carbonate rocks and present seasonally high discharges.

Methodology

Land use mapping

A Landsat 7+TM image has been used for land use mapping in combination with the image analysis component of ArcView package (GIS). The image has been

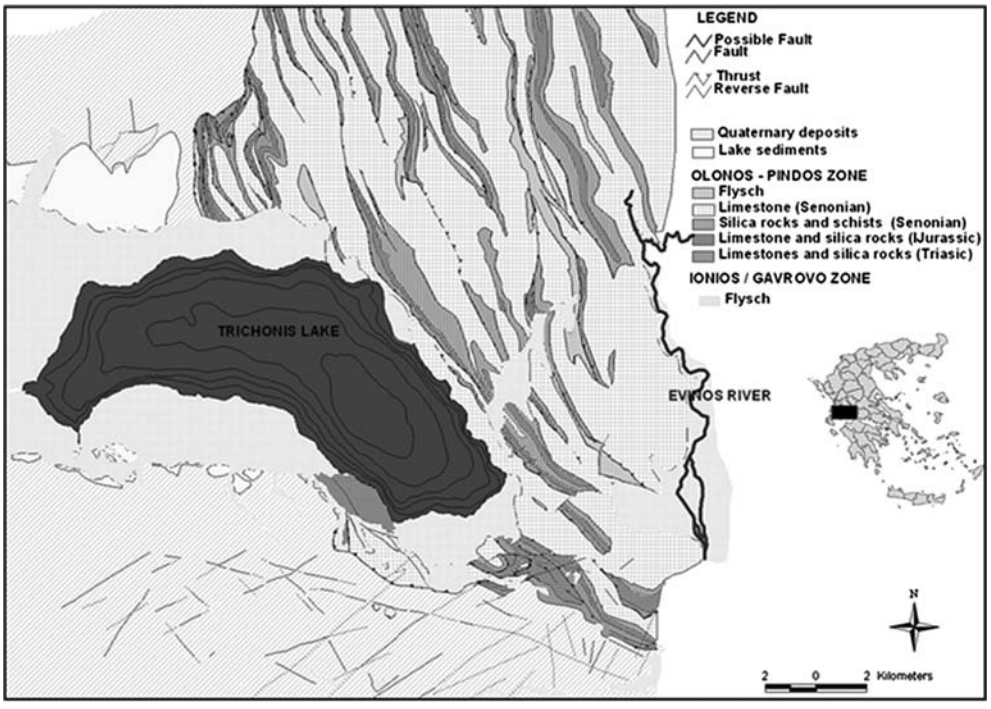

Fig. 1 Geologic map of Trichonis lake catchment

imported in the software and a georeference process followed in GGRS_87 coordinate system. A supervised classification approach has been implemented with the contribution of ISODATA algorithm to classify the image into different land categories based on field surveys and existing orthophoto maps.

The ISODATA algorithm is a widely used iterative mathematical function for such purposes in which classification of image pixels occur by splitting and merging of clusters according to their spectral signatures. The final number of clusters is given by the user while the objective is to minimize the variability within each cluster and therefore minimize the mean squared error (MSE):

$$\mathrm{MSE} = \frac{\sum_{\forall x} [x - C(x)]^2}{(N - c)^b} \quad (1)$$

where N is the number of pixels, C indicates the number of clusters and b is the number of spectral bands.

For the scope of this study four land cover categories have been chosen/selected including (1) agricultural fields, (2) forest, (3) urban areas and (4) open water that has been later excluded from the risk mapping process. The resultant map has been validated through existing orthophoto maps and relevant information acquired by the local authorities. The extent of each land category has been accurately quantified by utilizing spatial analyst module of the ArcView program. The developed land use map has been further elaborated in the next stages of this study to provide the hazard map of the area.

Isotopic study

The isotopic study of the broader area was conducted by collecting water samples from 25 specific points of interest, including springs, streams and the lakes, on a wide spatial distribution (Fig. 2). Initially, the values of electric conductivity (mS/cm) were recorded in most of the sampling locations, as well as their exact coordinates and altitude with the use of GPS equipment.

Four seasonal sampling efforts have been attempted (May, July, September and December 2003) with the collaboration of experts from the isotopic hydrology laboratory of "NCSR Demokritos" research center. The equipment used for this analysis was a mass spectrometer with which the ratio $^{18}O/^{16}O$ in relation to the Vienna standard for mean oceanic water (VSMOW) was estimated ($\delta^{18}O$):

$$\delta^{18}\mathrm{O} = \frac{(R_{\mathrm{sample}} - R_{\mathrm{VSMOW}})}{R_{\mathrm{VSMOW}}} \times 10^3 \quad (2)$$

(Perrin et al. 2003), where R_{sample} is the $^{18}O/^{16}O$ in the sample, R_{VSMOW} is the $^{18}O/^{16}O$ in the Vienna standard for mean oceanic water.

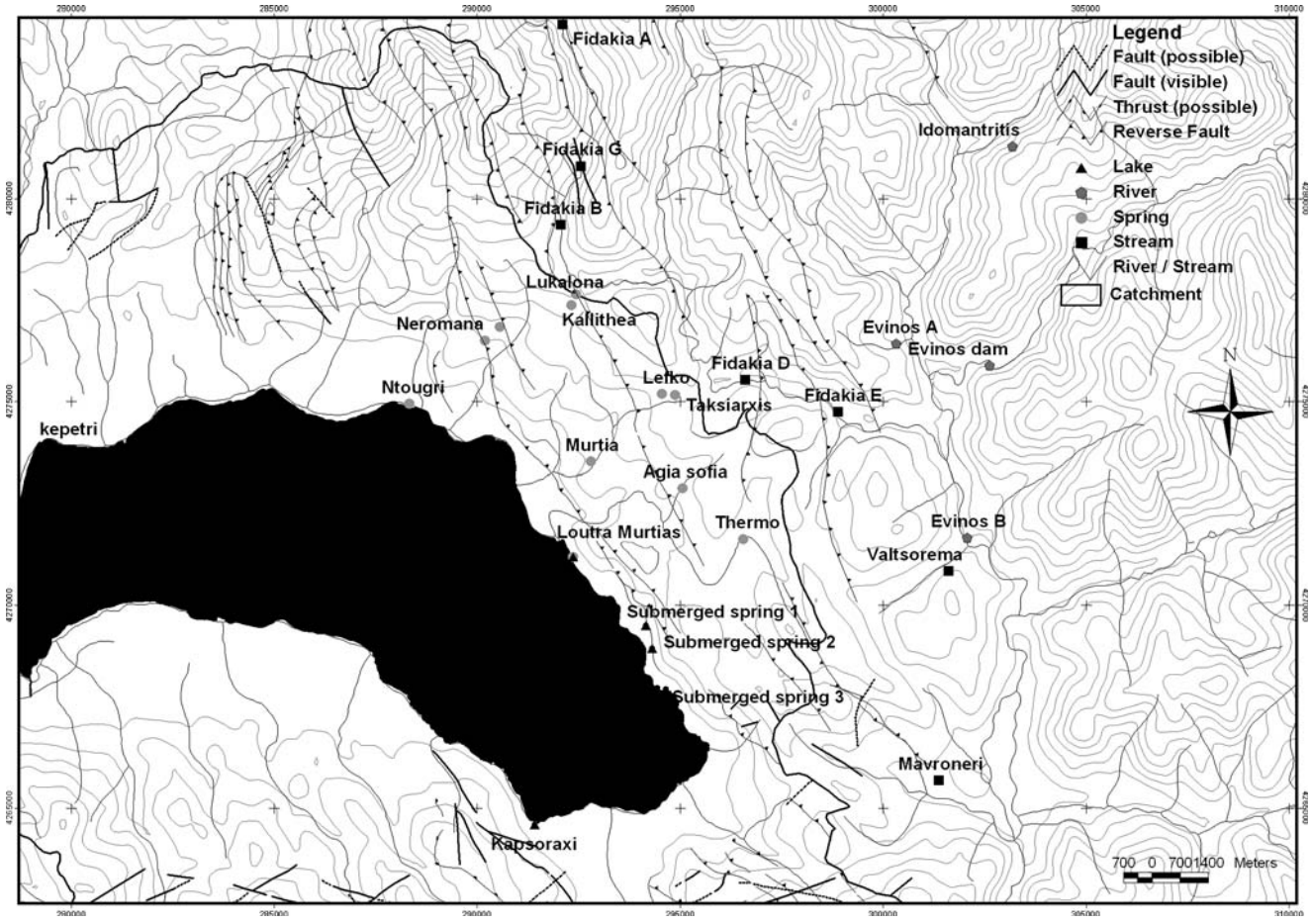

Fig. 2 Sampling locations and tectonic features in the study area

Statistical analysis of the $\delta^{18}O$ values was undertaken for detecting their temporal and spatial variation, as well as their changes in different altitudes of the study area. This process allowed the estimation of potential recharge altitudes for each sampling location. The isotopic values have been projected onto the geotectonic map of the area and a combination of quantitative and qualitative analysis allowed to develop clusters of sampling locations comprising discharge points of common recharge origins. Electric conductivity measurements of the most significant springs and the lake were also taken into consideration and were combined with the aforementioned analysis in order to facilitate the physical interpretation of the results. The outcome of this study provided information about the groundwater preferential flowpath directions in the broader area and potential interactions between various water bodies that have been then used in the development of the local vulnerability map.

Groundwater vulnerability and risk mapping

The vulnerability mapping effort followed the specifications suggested by the EU project, Cost Action 620 (Adams et al. 2003), aiming at the protection of carbonate aquifers at a European level. All the analysis and mapping processes were conducted with the use of ArcView package and the spatial data was transformed into a grid format (25 m × 25 m size) facilitating map calculations. Initially, three maps describing the flow regime of the catchment (*C* map), the overlaying protective cover of the aquifer (*O* map) and the precipitation factor (*P* map) were developed. In the aforementioned methodology, a *K*-factor is also stated describing the karst network of the study area that is used when source (e.g., drinking well) vulnerability assessment is required (Adams et al. 2003). In the particular effort, this parameter has been excluded, as suggested in the aforementioned method, since the aim is to assess the intrinsic vulnerability and risk of the entire groundwater body of the study area. Specifically, the detailed geologic map as well as the soil data obtained from recent hydrogeologic surveys in the area (Zacharias et al. 2003) have been used for the

development of the map representing the overlaying protective layers function of the groundwater in the study area (O map). Particularly, the thickness of soil horizons and geologic formations in the study area has been estimated through geological cross sections and validated while the spatial distribution as well as the type of lithology and soil texture have been acquired by existing geological maps of the Institute of Geological and Mineralogical Exploration. For the necessary hydrogeological information such as permeability categories and aquifer's confinement condition recent relevant studies of the particular area have been used (Zacharias et al. 2003). Topographic maps of 1:25,000 scale have been also acquired by the Hellenic Geographic Military Service, imported in Arcview software and elaborated with the 3D analyst component to develop initially the digital elevation model (DEM) of the area and then the respective slope map.

The O map describing the soil protective function was developed in the first stage by assigning values from one in areas of low soil protection (sandy soils with less than 1 m depth) to five in zones of high protection (clayey soils with depth more than 1 m). In areas with no soil present, the value 0 was assigned. The O_l map was then developed describing the protection originating from the lithology of the study area by classifying zones of high protection (clays, silts and marls: value 5) to formations of low protective function (karstic rocks: value 1). The overlaying protection layers map (O map) has been then calculated:

$$O_{\text{map}} = O_l + O_s \tag{3}$$

The concentration of flow map (C map) has been produced by taking into account the degree of karst development in the particular area, the slope map, the results from the isotopic analysis and the existence of vegetation, which reduces the velocity of surface runoff. Therefore, areas with well developed karst, low slopes and absence of vegetation were classified as having high reduction of protection since they are prone to pollution while areas with absence of karstic features such as high slopes and vegetation present low potential of direct infiltration and pollution intrusion. In this assessment, the outcome from the isotopic study has been used to describe the areas of preferential groundwater movement and assign the appropriate index values.

The precipitation factor map (P map) was developed by estimating the rainfall intensity of the study area (P_I) and the annual amount of rainfall (P_Q). For the particular study, 10-years data from five rain gauging stations, homogeneously distributed in Trichonis area, were used and spatially integrated with universal krigging method. The resulted P map has been calculated according to the equation:

$$P_{\text{map}} = P_Q + P_I \tag{4}$$

The aquifer's intrinsic vulnerability map was then developed by multiplying these three maps (C, O and P maps) in the ArcView environment, which provided the COP map representing the different vulnerability zones of the study area. The intrinsic vulnerability index for each grid varies from 0 (very high vulnerability) to 15 (very low vulnerability) while the index values grouping in five qualitative classes have been conducted according to the relevant methodology for reporting purposes.

For the development of the groundwater risk map hazard weighting values (H_i) have been assigned to each category of the already presented land use map of Trichonis catchment according to the COP methodology (Adams et al. 2003). The hazard weighting index used varies from 0 (very low hazard) to 100 (very high hazard) while intense agricultural practices were the most harmful land category of the particular area with a hazard value of 40. It should be stated that weighing the hazards originating from human activities is a difficult task with significant uncertainties but in this case special attention has been paid to the effects of toxicity, mobility and solubility of the potential contaminants.

Groundwater risk assessment was the final stage of this study and for this purpose the spatial distribution of hazard and intrinsic vulnerability indices developed before has been used. Thus, the associated risk map has been produced by the combination of the intrinsic vulnerability map and the hazard map according to the formula:

$$R_i = 1/H_i \times p \tag{5}$$

where R_i is the risk intensity index, H_i is the hazard index and p is the intrinsic vulnerability index as indicated in the COP map.

The produced vulnerability and risk maps have been evaluated and validated by attempting a physical interpretation of the different zones based on already existing hydrogeological information and maps.

Results

Land use mapping

The land cover map produced by the Landsat image analysis (Fig. 3) illustrates that forested lands dominate covering more than half of the area (57% of the total extent, Table 1), while cropland follow with 33%, extending over the lowland zone close to the lake where water abstraction schemes pumping directly from the lake exist. Built up areas do not overcome

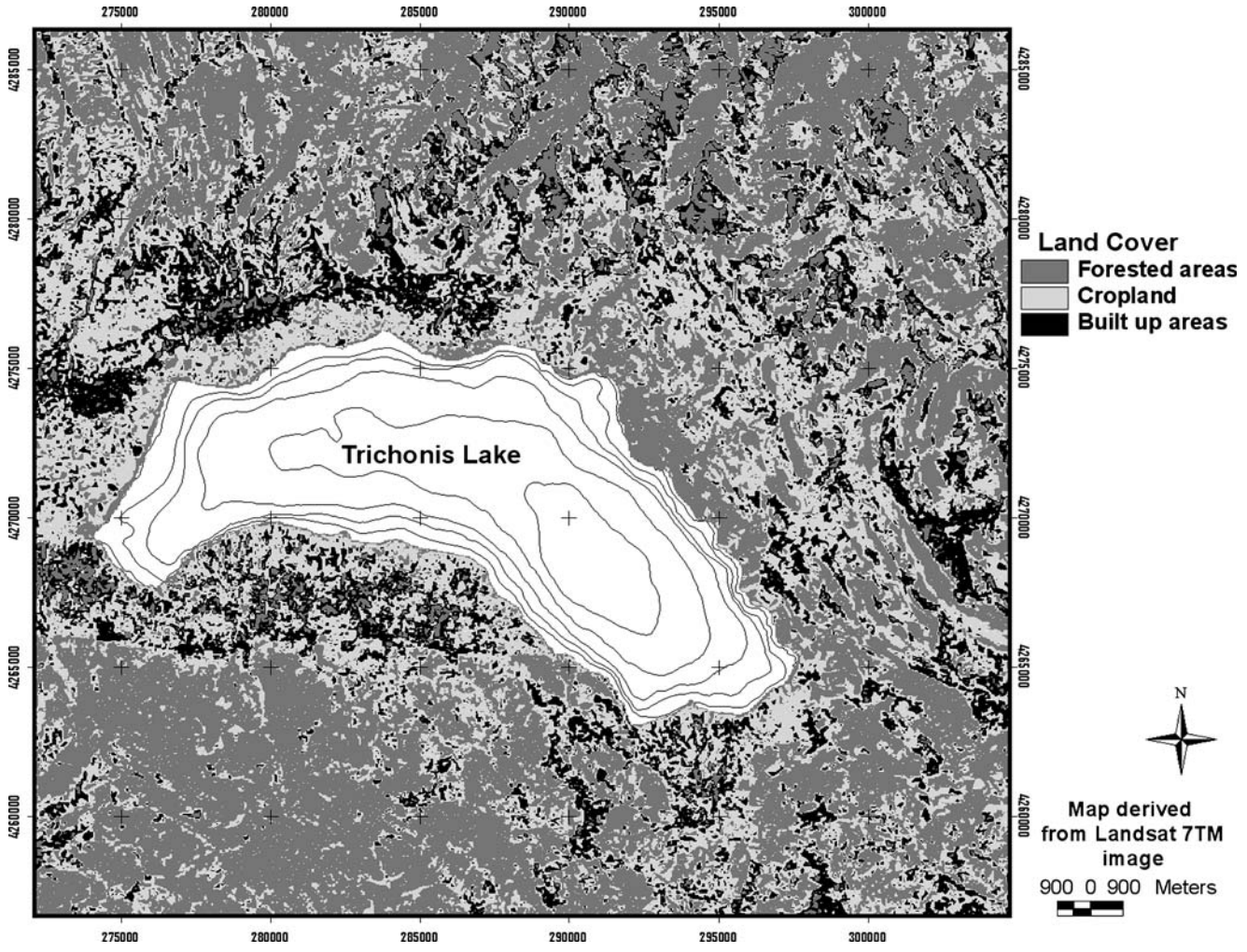

Fig. 3 Land cover map of the study area

10% of the study site which is relatively low but expected since the socioeconomic patterns of most rural areas in Greece in the last two decades indicate a very limited population density in such areas. No significant differences were observed in the land use categories extent of the produced map with land use maps of the previous decade and when associating the results with information derived from the local authorities. Such comparison also indicated very slow changes in the socioeconomic conditions of the area. Adding to this, orthophoto maps and recent aerial photos of the site were examined in order to validate the above land cover map by randomly selecting points of known land category in the pre-existing data and comparing them with the respective coverage of the map produced by the satellite image. The results from this analysis depicted a high accuracy in the produced map since in more than 95% of the selected points the land category coincided in both maps. The hazard map of the study area was then produced by assigning specific indices given by the Pan European methodology for groundwater risk map development (Adams et al. 2003) Thereafter, the $1/H_i$ map was produced in order to estimate the risk map (Eq. 3).

Table 1 Land cover map classes and the associated hazard indices

Class names	Hazard index (HI)	Opposite HI	Area (m^2)	Total (%)
Built up areas	3	0.33	71,720,627	10
Forested areas	1	1	417,933,013	57
Cropland	2	0.5	240,705,569	33
Total			730,359,208	100

Isotopic study

The springs of the area present high variation in their $\delta^{18}O$ values, since the minimum value is $-0.264‰$ and

the maximum value is −7.459‰ depending mainly on the different origins of the recharge water as far as altitude is concerned. The lake samples had very high $\delta^{18}O$ values (−0.341 to −0.021‰) which were expected since the intense evaporation affects the isotopic values significantly. The rest of the springs located in the mountainous part of the study area present relatively low values fluctuating from −6.099 to −7.459‰, and indicating recharge altitudes from 20 to 670 m above sea level.

Evinos river also indicated an important range in its $\delta^{18}O$ values in various segments, from −6,980 to −6.820‰ in its upstream part and −6.651‰ for the branch of Evinos that is recharged by an existing dam. A very important element is that the sampling point B of Evinos presented a highly negative value (−7.043‰) indicating the contribution of groundwater with a recharge area of a very high altitude (approx. 600 m) while the measurement point is only at 340 m elevation.

The categorization of the sampling points, illustrated in Fig. 4, correlates $\delta^{18}O$ values with their altitudes and provides three groups of sampling locations that have different recharge areas (Table 2). In the first and third group, the areas with the lowest and highest sampling altitudes are presented, respectively, which are considered as areas of local recharge. On the other hand, most sampling points belonging to the second group illustrate locations of remote recharge areas that probably coincide with high altitude mountainous areas. The recharge altitude of the second group can be approximated by estimating the slope of the best-fit-line describing the $\delta^{18}O$-altitude relation for the local recharge groups. The samples' $\delta^{18}O$ values have been projected on the recharge altitude axis with the use of the aforementioned line. In the particular study, the slope of the $\delta^{18}O$-altitude line is 0.49‰/100 m and this is in accordance with similar research efforts that indicate a respective value of 0.44‰/100 m in Eastern Macedonia (Leontiadis et al. 1996). Therefore, the estimated recharge altitudes for the second group have been calculated to be well higher than 500 m.

Fidakia stream presents a significant hydrogeologic interest since the influence of tectonics on its flow is apparent. It flows very close to the lake catchment on karstic formations and during the summer period there is significant reduction of its discharge between the sampling locations B and D that cannot be attributed only to evaporation. This is also accredited by the fact that water sampling could not occur in June 2003 from Fidakia D and E since the discharge was approximately zero while Fidakia B had relatively low δ^{18}O value (−7.018‰). Thus, there are many possibilities that an interaction between the springs of the second group (Table 2, Fig. 2) and part of Fidakia stream between the sampling locations Fidakia B and D exists.

Regarding the temporal variation of δ^{18}O values, Fig. 5 shows that springs Ntougri and Neromana have almost identical isotopic values and temporal fluctuations indicating that they also have a common recharge area. Furthermore, the same pattern is observed for the springs of Agia Sofia and Mytria (Fig. 6) while slight differences in their absolute values could be due to a low-scale mixing and evaporation processes in the discharge area.

The upstream part of Fidakia torrent (point A) illustrates relatively low $\delta^{18}O$ values with small seasonal

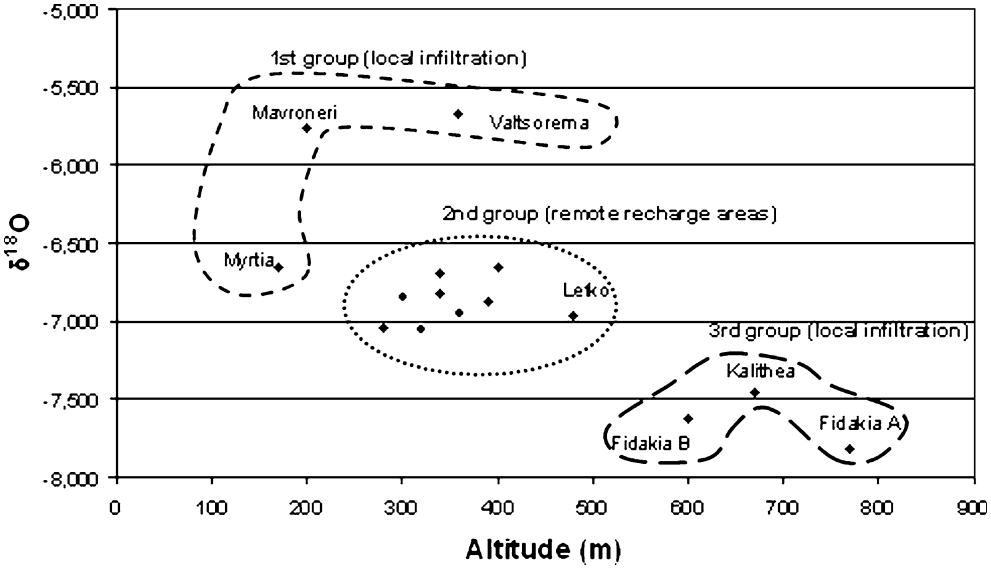

Fig. 4 Scatter diagram of sampling altitudes against recharge altitudes for the sampling locations indicating three groups of sampling locations in relation to their recharge areas

Table 2 Clusters of sampling locations indicating different recharge areas and their altitudes

Classification	Sampling location	*X*	*Y*	*Z*	$\delta^{18}O$ (05/2003)	$\delta^{18}O$ (07/2003)	$\delta^{18}O$ (09/2003)	$\delta^{18}O$ (11/2003)	$\delta^{18}O$ (12/2003)	Water body
First group	VALTSOREMA	301,633	4,270,851	360	−5.672	−5.701				River/stream
	MAVRONERI	301,385	4,265,682	200	−5.769					> >
	MYRTIA	292,815	4,273,534	170	−6.659	−6.351	−6.518	−6.470	−6.615	Spring
Second group	AGIA SOFIA	295,067	4,272,887	320	−7.055	−6.448	−6.676	−6.632	−6.623	Spring
	LEFKO	294,553	4,275,190	480	−6.967	−6.988	−6.923			> >
	NEROMANA	290,566	4,276,837	390	−6.876	−6.857	−6.867	−6.988	−6.993	> >
	EVINOS A	300,314	4,276,428	340	−6.820	−6.466	−6.703	−6.728	−6.466	River/stream
	EVINOS B	302,074	4,271,672	280	−7.043	−6.876	−7.175	−6.911	−6.843	> >
	FIDAKIA D	296,618	4,275,535	360	−6.951			−7.071	−7.121	> >
	FIDAKAI E	298,906	4,274,746	300	−6.841			−7.037	−6.890	> >
	EVINOS DAM	302,615	4,275,896	400	−6.651					River/stream
	THERMO	296,559	4,271,637	340	−6.687	−6.587	−6.445	−6.713	−6.718	> >
Third group	KALITHEA	292,443	4,277,651	670	−7.459	−6.498	−7.022	−7.106		
	FIDAKIA B	292,085	4,279,368	600	−7.629	−7.018	−6.983		−7.293	River/stream
	FIDAKIA A	292,120	4,284,308	770	−7.816	−7.507	−7.561	−7.837	−7.459	> >

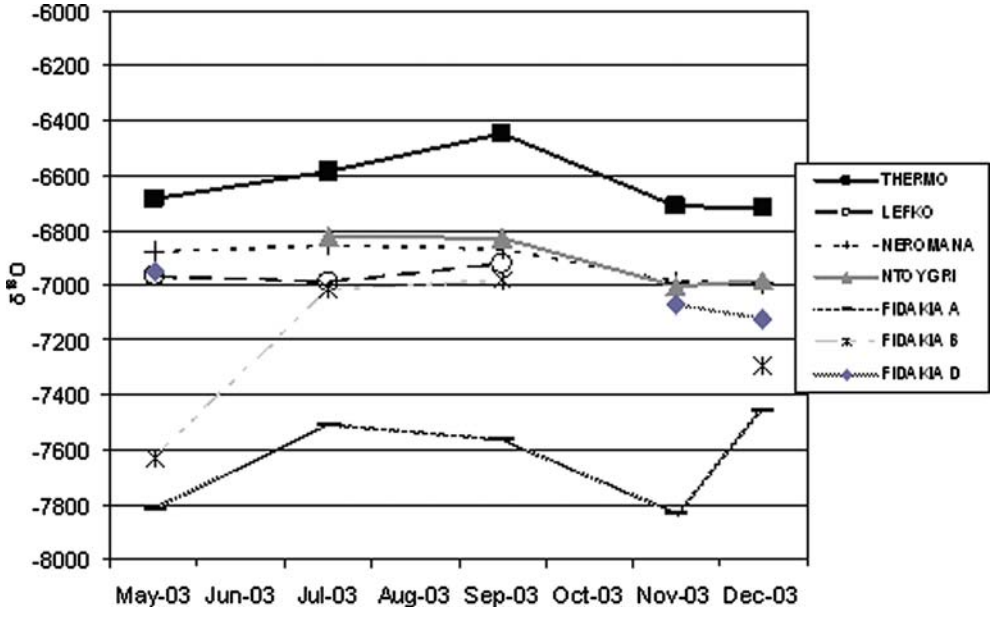

Fig. 5 Temporal variation in the $\delta^{18}O$ values of sampling locations for the period 05/2003–12/2003

fluctuations due to its mountainous conditions (over 800 m) facilitating local infiltration and eliminating isotopic degradation from evaporation effects. This pattern is not followed in the downstream parts because of the mixing processes between local and remotely originated water and the temperature effect that increase the $\delta^{18}O$ values.

As stated above, Evinos river downstream (point B) has particularly lower $\delta^{18}O$ values than upstream (point A). Additionally, the values in point A are lower during the period September–December 2003, whereas in point B they are higher during the same period. These observations lead to the conclusion that the upstream part of Evinos receives mainly surface water of local origin, whereas significant groundwater recharge from high altitudes affect its downstream part (Evinos B).

A group of springs in the study area (Kallithea, Myrtia, Ag. Sofia and Thermo) are strongly affected by the seasonal changes in temperature since their isotopic values increase during the summer period. This indicates that these springs are mainly recharged by medium altitude surface water bodies (approx. 500–550 m) which are also affected by seasonal temperature variations. The

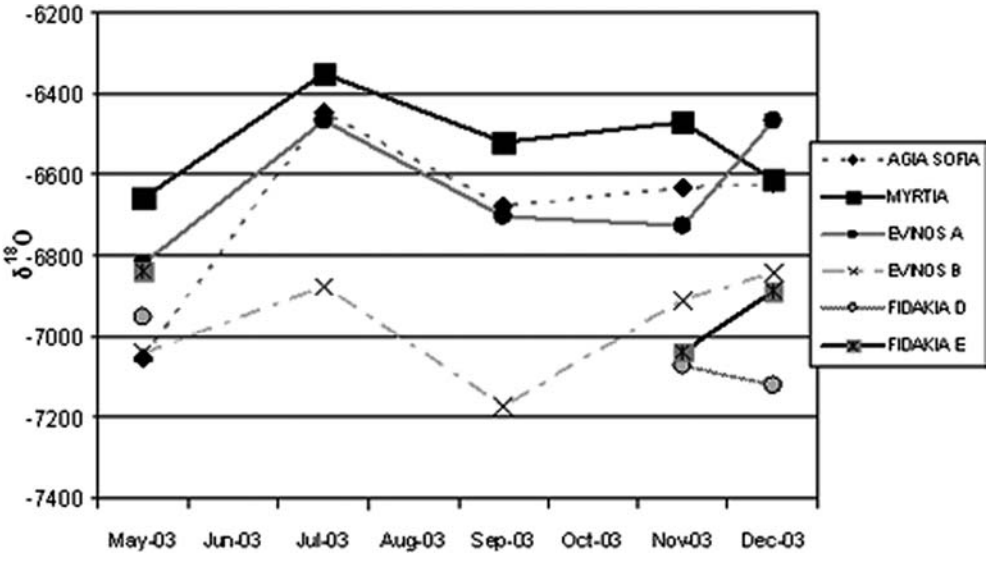

Fig. 6 Temporal variation in the $\delta^{18}O$ values of sampling locations for the period 05/2003–12/2003

western part of Fidakia stream could be a potential supplier for the above springs since it is the main surface water body in the particular area and the observed thrusts and faults along its flow on karstic formations, with NW–SE direction, can well explain high local infiltration and discharge in the particular spring locations.

The rest of the springs in Trichonis catchment (Ntougri, Neromana, Lefko and Lykalona) maintain relatively low isotopic values during the entire sampling period (−6.825, −6.857, −6.988 and −7.202‰ respectively), which means that their recharge area is not significantly influenced from seasonal temperature alterations and therefore high altitude surface water bodies could serve as their supplier.

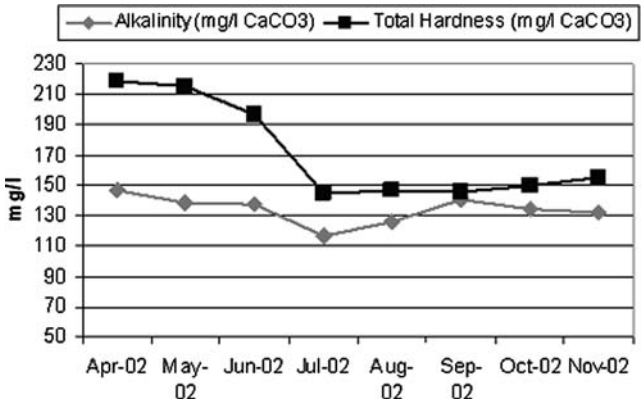

Fig. 7 Alkalinity and hardness in Trichonis lake during the study period

The significant groundwater recharge in the lake from remote areas and particularly from the snowmelt of Panaitoliko mountain through Fidakia stream is also validated by the monthly monitoring of chemical parameters such as alkalinity and total hardness in the lake. Moreover, a significant decrease of alkalinity and total hardness is observed during the period May–July 2002 (Fig. 7) in the storages of the lake as a result of the 'new' water introduced in the reservoir through the groundwater recharge process that has relatively low Ca^{++} and Mg^{++} values. Additionally, the extended travel times imposed by the remote sources of groundwater recharge are also accredited by Fig. 7, since snowmelt in the area ends by late May each year while the low peak of the above chemical parameters which indicates elimination of the groundwater component in the lake is observed at the end of July (approx. 2 months travel time). Thus, the primary groundwater flow direction coincides with the tectonic features of the eastern part of the study area (NW–SE, Fig. 8) while there is also a secondary preferential flowpath with perpendicular direction (NE–SW) that explains the discharge of varions karstic springs along the eastern lakeshore.

Vulnerability mapping

The *C* map (Fig. 9) illustrates the potential decrease of groundwater protection as a result of the flow regime toward the aquifer. Thus, the areas classified as having a very high decrease of protection facilitate the pollutants flow to the groundwater body. These zones are encountered around the main tectonic features of the

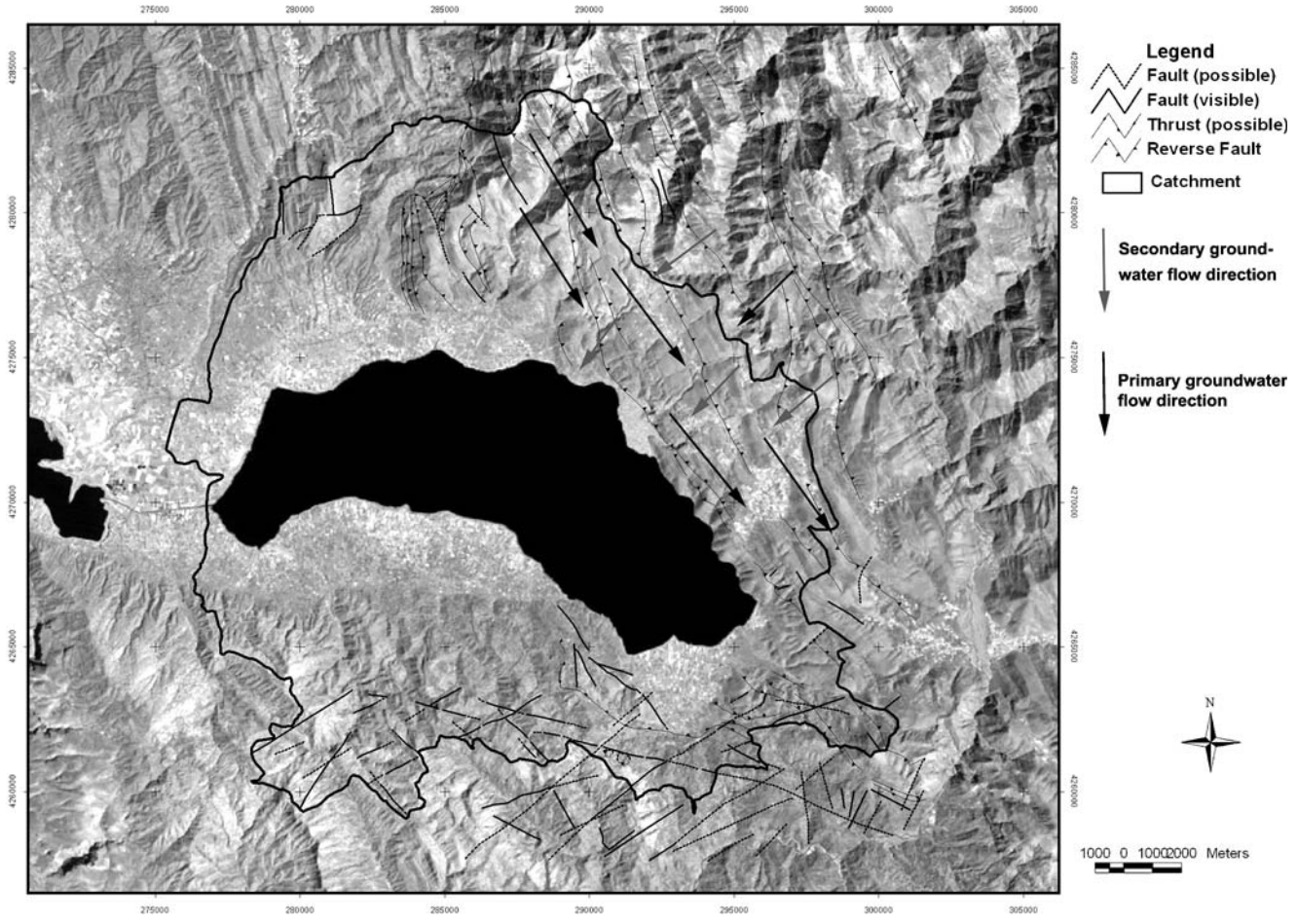

Fig. 8 Primary and secondary groundwater flow directions in the broader area of Trichonis lake

study area (reverse faults and thrusts) presenting a direction of NW–SE and occur in the eastern part of the examined site on calcareous formations. Most of the study site has a moderate decrease of protection because of the impermeable flysch formations. The dense vegetation dominating the western part of the site obstruct fast infiltration while in the eastern part the Senonian pelagic Limestone blocks cause moderate reduction of groundwater protection. The highly tectonized areas coinciding with the Jurassic limestones create a high reduction of protection in the groundwater resources since they facilitate fast flow towards the aquifer and interact strongly with the groundwater movement according to the isotopic study.

The *O* map of the area (Fig. 10) presenting the protection of overlaying layers to the aquifer is in agreement with the geological and *C* maps since in the eastern part of the catchment, where high slopes and calcareous rocks exist, the depth of soil is limited and therefore the associated protection is low. In the southern and western parts of the study area where the thickness of soil is over 1 m and in the lowland zone may even reach values of 50 m, with materials that fluctuate from low to medium permeability, the protection is high. Nevertheless, the highly tectonized areas that coincide to preferential groundwater flowpaths in combination with the absence of soil depict the lowest protection values for the aquifer.

The vulnerability map of the area (COP map, Fig. 11) indicates that a significant proportion of the study area (31%, Table 3) is classified as having high and very high vulnerability to groundwater pollution while only 25% of the area can be considered as of low vulnerability. The zones of high and very high groundwater vulnerability represent the calcareous formations in the northeastern part of the examined site and particularly the highly tectonized, karstic formations that facilitate groundwater movement as revealed from the isotopic study. The reverse faults and thrusts contribute significantly to the potential

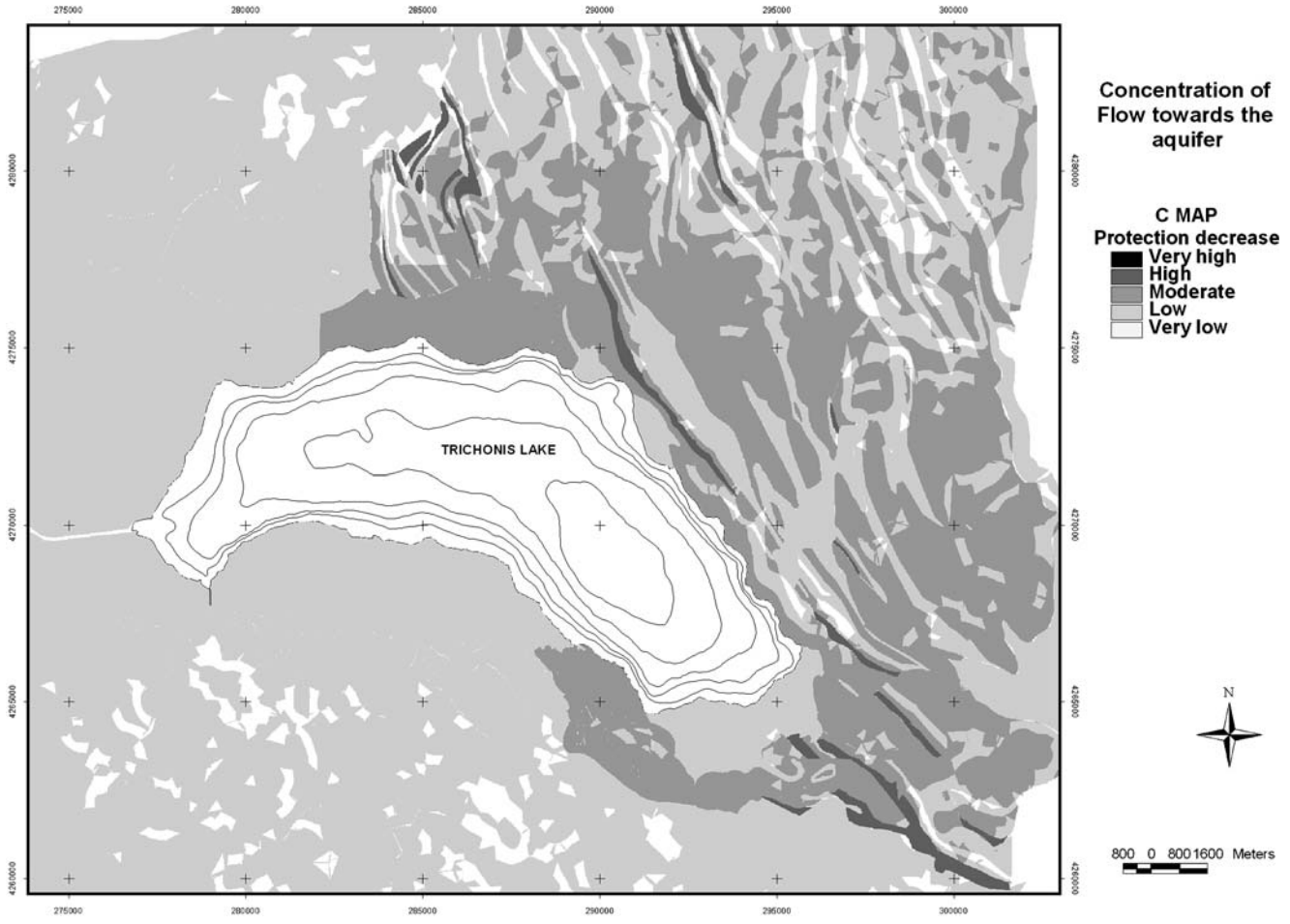

Fig. 9 Concentration of flow map (*C* map) for the study area

fast pollution flow to the aquifer while their proximity to Trichonis Lake introduces high relevant risks for this freshwater body. The western part of the study area with the flysch formations and the sediments around the lake illustrates moderate vulnerability (45% of the examined area) as a result of the natural attenuation regime of this zone while the flysch formations of the southern part indicate a low vulnerability value due to the absence of significant aquifers in this particular area.

The combination of the intrinsic vulnerability map and the hazard map provided the groundwater pollution risk map of the study area (Fig. 12). This process introduces the socioeconomic component in the concept of intrinsic vulnerability for groundwater pollution which is based only on scientific criteria. This integrates the whole process leading to the assessment of aquifer's pollution risk, a very important element for decision making and planning.

The sites characterized as of high and very high pollution risk cover 40% of the study area (Table 4), whereas the ones of low and very low risk zones comprise only 35%. In the high and very high pollution risk areas, calcareous dominated zones are mainly included while the built up areas around the lake, laying on sedimentary and flysh formations, are also incorporated. The moderate risk zones involve areas mainly occupied by cropland in close proximity to the lake while the forested areas on flysch formations in the southwestern part of the area are classified as of low risk. Therefore, this map indicates that human activities producing pollutant substances in the central part of the study area and particularly north and east from Trichonis lake could have detrimental impacts on the water quality of the aquifer, as well as of the lake. However, there are limited zones in this northeastern part of the examined site that comprise mainly impermeable schists which could be possibly used for developmental actions associated to waste products. Nevertheless, attention should be paid to avoid installations close to the highly tectonized zones of

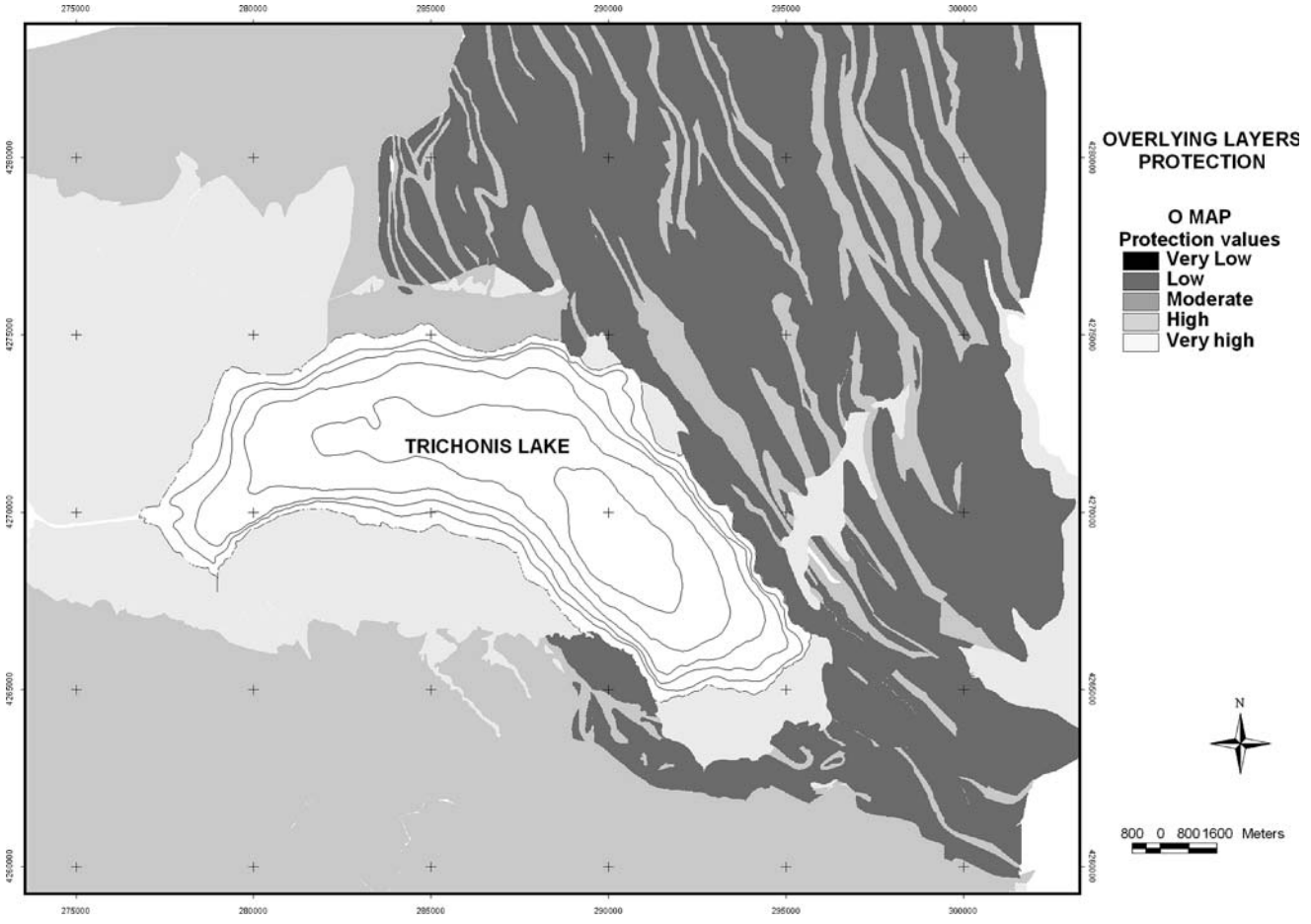

Fig. 10 Overlaying soil protective layers map (*O* map)

preferential groundwater flow that are classified as of high pollution risk (Fig. 12).

Discussion

The results of this study indicated that groundwater vulnerability and risk mapping is an efficient tool significantly assisting in planning and decision making processes. However, it demands accurate and detailed input data and therefore its efficiency increases when advanced complementary techniques are used such as isotopic analysis, remote sensing and GIS. The particular area illustrated high and very high vulnerability at a significant percentage of the examined coverage (31%) due to the dominant hydrogeologic conditions that comprise highly tectonized, calcareous formations with preferential flowpaths along discontinuities, fractures and reverse faults mainly in the NW–SE direction. Additionally, the lack of a sufficiently protective soil layer and the large slopes occurring in this particular part of the study area enhance the unfavorable conditions for the aquifer vulnerability. The sedimentary deposits around the lake present moderate vulnerability even though the relatively slow infiltration and high storage capacity facilitate natural attenuation of the potential pollutants. This is attributed to the interconnection of these deposits with the karstic aquifer increasing the possibility for pollution intrusion, hence the vulnerability class. The hazard map augmented the high and very high risk zones in the risk map (40% of the area) since the agricultural and most of the built-up areas existing around the lake on sedimentary deposits have been transferred in the high risk class. Moderate risk zones have been decreased (25%) in relation to the vulnerability map and cover only lowland areas on impermeable formations at a significant distance from the karstic aquifer while low and very low classes have increased their extent (35% of the site) mainly due to the existence of forested areas on the highland parts of the flysch formations.

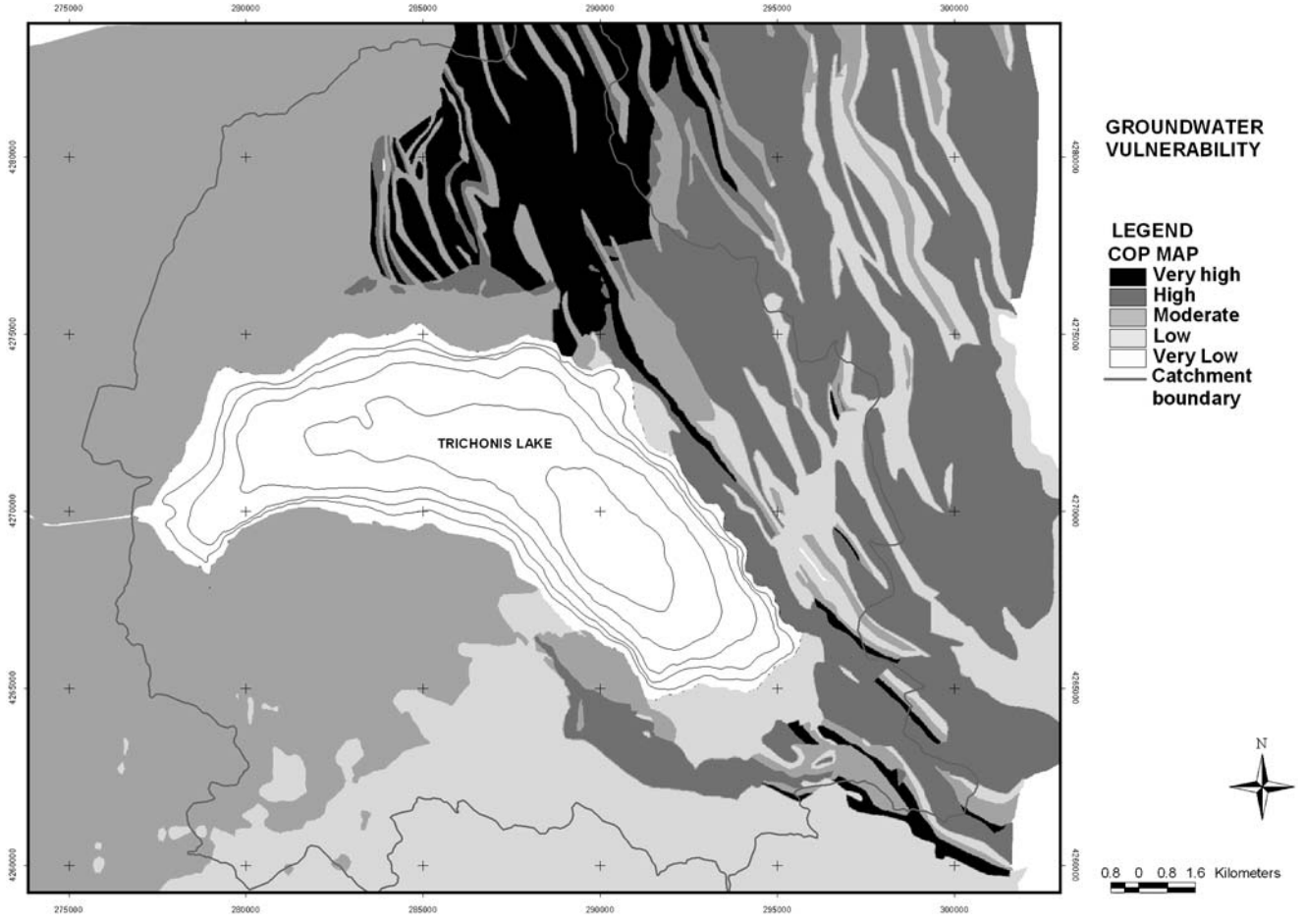

Fig. 11 Groundwater vulnerability map for the study area

Table 3 Vulnerability classes and extent

Vulnerability classes	Area (m^2)	Total (%)
Very high	55,310,922	8
High	164,653,605	23
Moderate	329,439,318	45
Low	181,933,430	25

The recently developed Pan European approach for groundwater vulnerability mapping (Adams et al. 2003) proved to be appropriate for the particular conditions of the study area since the produced vulnerability and risk maps were consistent with the local hydrogeologic regime and bibliographic data related to water quality. This method has also been used successfully in other areas and when compared to similar methodologies illustrates several advantages but also a drawback which is difficulty to validate vulnerability maps (Andreo et al. 2005). Several other studies attempting to map aquifer vulnerability have implemented different techniques such as the DRASTIC model developed by US EPA (Knox et al. 1993) that in some cases provided acceptable results (Rundquist et al. 1991; Al-Adamat et al. 2003; Babiker et al. 2005) while in other studies important shortcomings have been observed (Fritch et al. 2000; Dixon 2005). One of the most commonly encountered inconsistencies in vulnerability mapping applications, especially in complex geological settings such as karstic formations, is the classification of impervious areas to low vulnerability class even when interaction with karstic aquifers exist through overland and lateral flows. COP method takes into account this issue through the concentration of flow map (Andreo et al. 2005). Nevertheless, modifications of pre-existing methods are attempted during the last decade and improvements of the vulnerability and risk mapping methodologies occur that will eventually lead to an important decision support

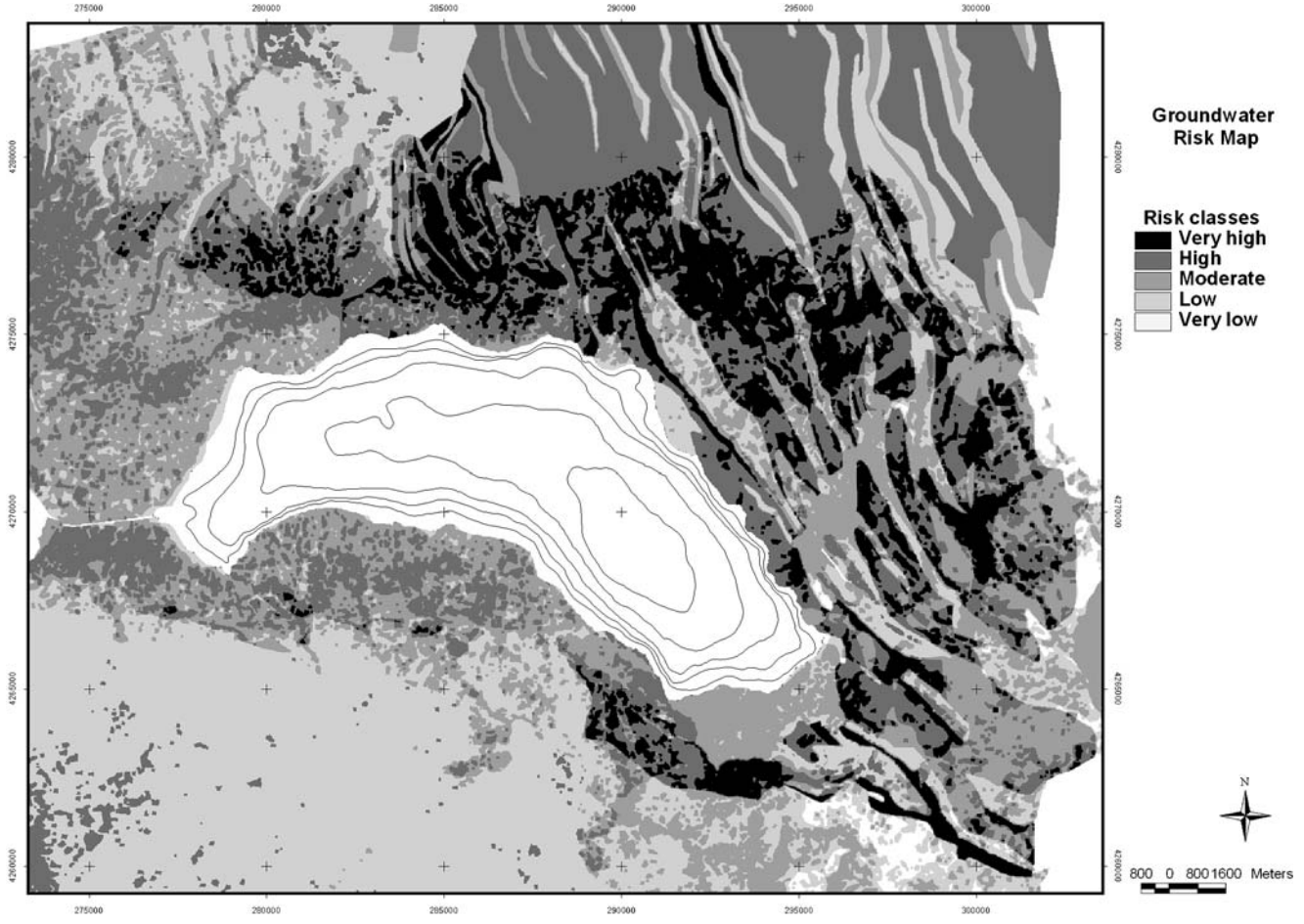

Fig. 12 Groundwater risk map

Table 4 Groundwater risk classes and associated extents

Risk classes	Area (m^2)	Total (%)
Very high	72,319,987	10
High	220,227,955	30
Moderate	181,488,255	25
Low	244,879,836	33
Very low	12,333,073	2

tool for groundwater protection and management as requested by the contemporary legislative framework worldwide.

Acknowledgments This study was conducted under the Life-Nature 1999 project entitled: 'Actions for the preservation of Calcareous fens in Trichonis lake'.

References

Adams B, et al (2003) Vulnerability and risk mapping for the protection of carbonate (Karst) aquifers. In: Zwahlen (ed.). Cost action 620, Final report, p 297

Al-Adamat RAN, Foster IDL, Baban SMJ (2003) Groundwater vulnerability and risk mapping for the Basaltic aquifer of the Azraq basin of Jordan using GIS. Remote sensing and DRASTIC. Appl Geogr 23:303–324

Andreo B, Goldscheider N, Vadillo I, María Vías J, Neukum Ch, Sinreich M, Jiménez P, Brechenmacher J, Carrasco F, Hötzl H (2005) Karst groundwater protection: first application of a Pan-European approach to vulnerability, hazard and risk mapping in the Sierra de Líbar (Southern Spain). Sci Total Environ (in press)

Babiker SI, Mohamed MA, Hiyama T, Kato K (2005) A GIS-based DRASTIC model for assessing aquifer vulnerability in Kakamigahara Heights, Gifu Prefecture, central Japan. Sci Total Environ 345:127–140

Diazconti Carreón C, Nelson S, Mayo A, Tingey D, Maren S (2003) A mixed groundwater system at Midway, UT: discriminating superimposed local and regional discharge. J Hydrol 273(1–4):119–138

Dixon B (2005) Groundwater vulnerability mapping: a GIS and fuzzy rule based integrated tool. Appl Geogr 25:327–347

Finch WJ (1997) Estimating direct groundwater recharge using a simple water balance model—sensitivity to land surface parameters. J Hydrol 211:112–125–1998

Fritch TG, McKnight CL, Yelderman JC Jr, Arnold JG (2000) An aquifer vulnerability assessment of the paluxy aquifer, central Texas, USA, using GIS and a modified DRASTIC approach. Environ Manage 25:337–345

Goldscheider N, Klute M, Sturm S, Hotzl H (2000) The PI method: a GIS based approach to mapping groundwater vulnerability with special consideration of karst aquifers. Z Angew Geol 46(3):157–66

Hussain N, Church TM, Kim G (1999) Use of 222-Rn and 226-Ra to trace groundwater discharge into the Chesapeake Bay. Mar Chem 65:127–134

Jeannin Y, Hauns MP, Atteia O (2001) Dispersion, retardation and scale effect in tracer breakthrough curves in karst conduits. J Hydrol 241(3–4, 31): 177–193

Jones I, Banner J (2003) Estimating recharge thresholds in tropical karst island aquifers: Barbados, Puerto Rico and Guam. J Hydrol 278(1–4, 25) 131–143

Knox RC, Sabatini DA, Canter LW (1993) Subsurface transport and fate processes. Lewis Publishers, USA

Leontiadis IL, Vergis S, Christodoulou Th (1996) Isotope hydrology study of areas in Eastern Macedonia and Thrace, Northern Greece. J Hydrol 182:1–17

Rundquist DC, Peters AJ, Liping D, Rodekohr DA, Ehrman RL, Murray G (1991) State-wide groundwater vulnerability assessment in Nebraska using the DRASTIC/GIS model. GeoCartogr Int 6:51–58

Swarzenski PW, Reich CD, Spechler RM, Kindinger JL, Moore WS (2001) Using multiple geochemical tracers to characterize the hydrogeology of the submarine spring off Crescent Beach, Florida. Chem Geol 179(1–4):187–202

Vias JM, Andreo B, Perles MJ, Carrasco F, Vadillo I, Jimenez P (2002) Preliminary proposal of a method for vulnerability mapping in carbonate aquifers. In: Carrasco F, Duran JJ, Andreo B (eds) Second Nerja Cave Geol Symp Karst and Environment, 20–23 October 2002, Nerja, Spain, p 75–83

Vrba J, Zoporozec A (1994) Guidebook on mapping groundwater vulnerability. IAH International Contribution for Hydrogeology, vol 16. Hannover7 Heise, p. 131

Zacharias I, Dimitriou E, Koussouris Th (2003) Estimating groundwater discharge into a lake through underwater springs by using GIS technologies. Environ Geol J 44(7):843–851